



# Vertical liquid controlled adiabatic waveguide coupler

HERBERT D'HEER,<sup>1</sup> KUMAR SAURAV,<sup>2</sup> WEIQIANG XIE,<sup>1,3</sup> CRISTINA LERMA ARCE,<sup>2</sup> JAN WATTÉ,<sup>2</sup> AND DRIES VAN THOURHOUT<sup>1,\*</sup>

<sup>1</sup>Photonics Research Group, Department of Information Technology (INTEC), Ghent University – imec, 9052 Gent, Belgium

<sup>2</sup>CommScope, 3010 Kessel-Lo, Belgium

<sup>3</sup>Currently with the Department of Electrical and Computer Engineering, University of California, Santa Barbara, California 93106, USA

\*dries.vanhourhout@ugent.be

**Abstract:** A broadband vertical liquid controlled optical waveguide coupler (LCC) is demonstrated. The fabricated vertical LCC with silicon nitride (SiN) waveguides can switch light between 2 stacked photonic circuit layers with zero energy consumption in a steady switch state. In combination with low-loss interlayer waveguide crossovers they enable large scale non-volatile switch circuits with low loss. The fabricated vertical LCC has a loss less than 2.0 dB in bar state and less than 2.6 dB in cross state over the telecommunication wavelength range 1260 nm to 1630 nm. Interlayer waveguide crossovers with the same interlayer oxide thickness as the LCC have a loss less than 0.06 dB over the same wavelength range. The crosstalk of the LCC is less than -21 dB over the wavelength range 1500 nm to 1630 nm for both bar and cross state.

© 2018 Optical Society of America under the terms of the [OSA Open Access Publishing Agreement](#)

**OCIS codes:** (060.2330) Fiber optics communications; (130.4815) Optical switching devices; (230.4170) Multilayers; (230.7370) Waveguides; (250.5300) Photonic integrated circuits.

## References and links

1. K. Tanizawa, K. Suzuki, K. Ikeda, S. Namiki, and H. Kawashima, "Non-duplicate polarization-diversity 8 × 8 Si-wire PILOSS switch integrated with polarization splitter-rotators," *Opt. Express* **25**(10), 10885–10892 (2017).
2. J. Chiles, S. Buckley, N. Nader, S. Woo Nam, R. P. Mirin, and J. M. Shainline, "Multi-planar amorphous silicon photonics with compact interplanar couplers," *APL Photonics* **2**(11), 116101 (2017).
3. K. Shang, S. Pathak, B. Guan, G. Liu, and S. J. B. Yoo, "Low-loss compact multilayer silicon nitride platform for 3D photonic integrated circuits," *Opt. Express* **23**(16), 21334–21342 (2015).
4. W. D. Sacher, Y. Huang, G. Q. Lo, and J. K. S. Poon, "Multilayer silicon nitride-on-silicon integrated photonic platforms and devices," *J. Lightw. Technol.* **33**(4), 901–910 (2015).
5. D. D. John, M. J. R. Heck, J. F. Bauters, R. Moreira, J. S. Barton, J. E. Bowers, and D. J. Blumenthal, "Multilayer platform for ultra-low-loss waveguide applications," *IEEE Photon. Technol. Lett.* **24**(11), 876–878 (2012).
6. S. Han, T. J. Seok, K. Yu, N. Quack, R. S. Muller, and M. C. Wu, "Large-scale polarization-insensitive silicon photonic MEMS switches," *J. Lightwave Technol.* **36**(10), 1824–1830 (2018).
7. S. Günther, C. Endrödy, S. Si, S. Weinberger, R. Claes, Y. Justo, H. D'heer, A. Neft, and M. Hoffmann, "EWOD system designed for optical switching," in *Proceedings of IEEE 30th Int. Conf. Micro Electro Mech. Syst.* (IEEE, 2017), 1329–1332.
8. H. D'heer, C. Lerma Arce, S. Vandewiele, J. Watté, K. Huybrechts, R. Baets, and D. Van Thourhout, "Nonvolatile liquid controlled adiabatic silicon photonics switch," *J. Lightwave Technol.* **35**(14), 2948–2954 (2017).
9. H. D'heer, K. Saurav, C. Lerma Arce, S. Tuccio, S. Clemmen, S. Lenci, A. Stassen, J. Watté, and D. Van Thourhout, "Broadband and temperature tolerant silicon nitride liquid controlled waveguide coupler," submitted to *J. Lightwave Technol.*
10. H. Ishikawa, "Fully adiabatic design of waveguide branches," *J. Lightwave Technol.* **25**(7), 1832–1840 (2007).
11. W. Xie, Y. Zhu, T. Aubert, S. Verstuyft, Z. Hens, and D. Van Thourhout, "Low-loss silicon nitride waveguide hybridly integrated with colloidal quantum dots," *Opt. Express* **23**(9), 12152–12160 (2015).
12. Cargille Laboratories, Inc., [www.cargille.com](http://www.cargille.com).
13. H. D'heer, K. Saurav, C. Lerma Arce, M. Detalle, G. Lepage, P. Verheyen, J. Watté, and D. Van Thourhout, "A 16 × 16 Non-Volatile Silicon Photonic Switch Circuit," *IEEE Photon. Technol. Lett.* **30**(13), 1258–1261 (2018).

## 1. Introduction

Large-scale photonic integrated switch circuits often require many waveguide crossovers to interconnect all switching elements. In polarization-independent switch circuits that use polarization diversity the number of waveguide crossovers is even larger [1]. Photonic integrated switch circuits could be used for example to reconfigure fiber-optic telecommunication networks. For such applications the switch circuit preferably has a very low insertion loss (IL) over the full telecommunication wavelength range from about 1260 nm to about 1630 nm. However, current single-layer waveguide crossovers have a loss contribution that is too high over this wavelength range.

A solution could be to stack photonic circuit layers such that waveguides do not need to cross in the same layer and such that the total IL of the switch can be reduced. This introduces the need of vertical photonic coupling elements that can transfer light between the different circuit layers. Low-loss vertical waveguide couplers have already been demonstrated [2–5]. A vertical coupler can also be designed to operate as a switch, reducing then the number of components in a switch circuit and the overall IL [6]. In the current paper we propose an elementary switch consisting of a vertical adiabatic waveguide coupler that can be actuated by liquids. The proposed vertical liquid controlled coupler (LCC) has a large bandwidth and can be non-volatile when integrated with for example an electrowetting-on-dielectric (EWOD) system. An EWOD system, such as the one shown in [7], allows to move droplets of a first liquid in a second liquid by applying appropriate actuation voltages and taking care the liquids are immiscible. If the actuation voltage is removed the droplets remain in place, facilitating the switch to operate with zero energy consumption in a steady state .

We discussed the operation principle of the LCC in detail before [8]. It consists of an adiabatic waveguide coupler, which has one of its waveguides exposed to a changeable liquid. The state of the switch depends on the refractive index of the medium that is present above the exposed waveguide. In [8] we also presented a first prototype of the LCC, using standard silicon photonics fabrication technology. These planar LCCs could operate with relatively good performance, but over a limited wavelength range. We showed that reducing the Si thickness could improve the performance of the LCC, and could also reduce the loss of waveguide crossovers. However, this also introduces the need for non-standard silicon-on-insulator (SOI) wafers with a sufficiently thick buried oxide layer.

The vertical LCC proposed in this paper consists of silicon nitride (SiN) waveguides. The use of SiN has several advantages over crystalline Si. First, it is easier to introduce a second waveguide layer by using chemical vapor deposition (CVD) technology than by using a second SOI wafer and a bonding and lapping process. Second, since the SiN is applied by a CVD process the thickness of the waveguides and SiO<sub>2</sub> cladding layers is highly flexible. Third, planar and vertical LCCs with SiN waveguides can also have better performance compared to LCCs with Si waveguides [9]. Light in SiN waveguides is less confined and has a larger overlap with the actuating medium above the waveguide. Therefore, the same variation in refractive index of the medium above the exposed waveguide introduces a larger variation in the effective refractive index for the SiN waveguide. This results in a better performance. The index contrast of SiN waveguides is still sufficiently large to achieve a fairly large refractive index variation as a function of waveguide width. This is also required to realize a good performance. Fourth, it is also worth to mention that the larger mode size in SiN waveguides can simplify the coupling strategy between the optical chip and optical fibers.

## 2. Design of vertical liquid controlled coupler

A schematic of the vertical LCC is shown in Fig. 1. It consists of 2 SiN waveguides that are stacked vertically with a SiO<sub>2</sub> layer in between. The adiabatic LCC is designed in a similar way

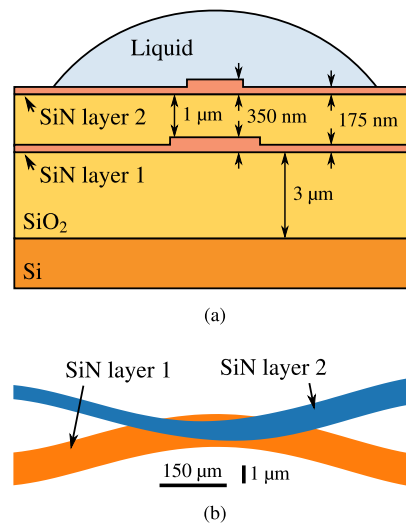


Fig. 1. Schematic of an LCC with (a) a cross section at the center and (b) a top view.

as described in [8]. As was described there the width of one waveguide is kept constant, while the width of the second waveguide and the center-to-center separation between both waveguides were optimised along the design guidelines outlined in [10] to maximise transmission and crosstalk over the whole wavelength range. The interlayer oxide thickness is taken as  $1.0\ \mu\text{m}$  and the actuating liquids have a refractive index of 1.37 and 1.55 at a wavelength of 1550 nm. The vertical distance between the two SiN layers should be sufficiently large to obtain interlayer waveguide crossovers with a low IL and crosstalk (XT) [3], but at the same time it should also be sufficiently small to achieve a high coupling efficiency of the LCC.

The simulated transmission of a  $900\ \mu\text{m}$  long LCC in bar and cross state is shown in Fig. 2 for different interlayer thicknesses. It can be noticed that the influence of the interlayer thickness on the transmission is smallest for the bar state. In cross state, the performance is better for a smaller interlayer thickness. An LCC in bar state with an interlayer thickness of  $1.0\ \mu\text{m}$  has an IL of 0.0 dB and XT less than  $-51\ \text{dB}$  over the wavelength range 1260 nm to 1630 nm. In cross state the IL and XT is less than 0.01 dB and  $-27\ \text{dB}$ , respectively, over the wavelength range 1500 nm to 1630 nm. Over the wavelength range 1260 nm to 1630 nm the IL and XT is less than 1.5 dB and  $-5\ \text{dB}$ , respectively. However, when the LCC would be used as part of a switch in a fiber-optic telecommunication network, a further improvement is preferred for wavelengths between 1260 nm and 1360 nm. The refractive index of the materials used in the simulation is 1.90, 1.47, and 1.44 for SiN, the interlayer oxide, and the bottom oxide, respectively, at a wavelength of 1550 nm (the material dispersion is taken into account in the simulations). The width of the bottom waveguide is  $2.0\ \mu\text{m}$  and the width of the top waveguide varies between  $0.9\ \mu\text{m}$  and  $1.6\ \mu\text{m}$  over its length. Waveguide losses are not included in the simulated transmission. Given their adiabatic nature, the couplers are in general relatively robust against fabrication tolerances. A misalignment between both waveguide layers in first order has the same effect as a change in the interlayer gap, as it impacts the waveguide to waveguide distance. Changes of the waveguide width typically result in a moderate shift of the transmission in the wavelength domain. In general the couplers can be made even more tolerant against fabrication variations by further increasing the length of the couplers.

The used fiber edge-couplers are tapered waveguides with a width that varies from  $1.5\ \mu\text{m}$  to  $2.6\ \mu\text{m}$  at the chip facets. The interconnecting waveguides and the waveguides in crossovers have

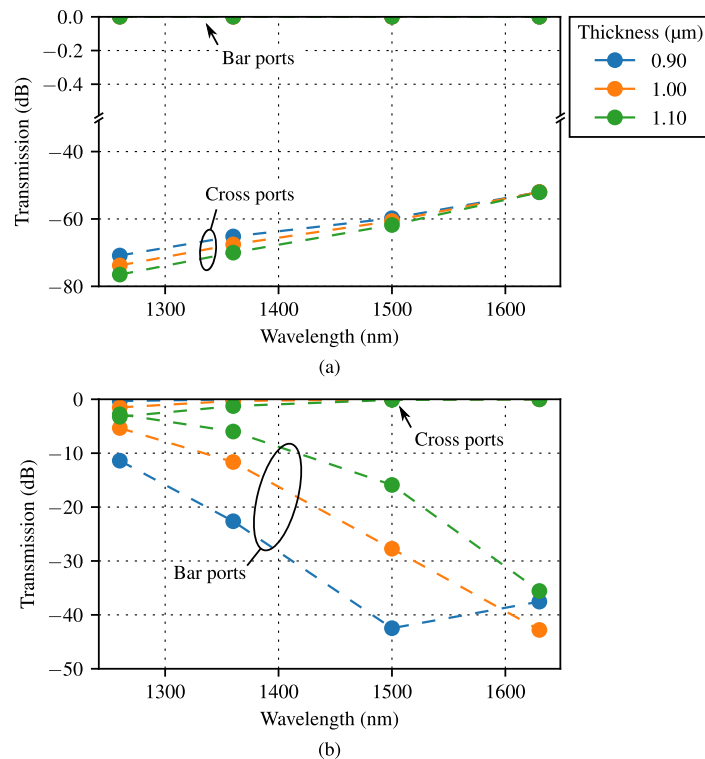


Fig. 2. Simulated transmission of a 900  $\mu\text{m}$  long vertical LCC in (a) bar state (with low refractive index on top of waveguide) and (b) cross state (with high refractive index on top of waveguide) for different interlayer oxide thicknesses.

a width of 1.5  $\mu\text{m}$ . The waveguide widths of the LCC are designed to be larger than 0.9  $\mu\text{m}$  such that the photonic circuit can be manufactured with a relatively low resolution lithography process.

### 3. Fabrication

Microscope images of fabricated vertical LCCs are shown in Fig. 3 and the fabrication process flow is shown in Fig. 4. As shown in Fig. 4(a), the fabrication starts with a thermally oxidized Si wafer with 3.0  $\mu\text{m}$  thick  $\text{SiO}_2$  on which a 350 nm thick SiN layer is deposited using plasma-enhanced chemical vapor deposition (PECVD) at 270°C. The waveguides in the first SiN layer are defined by optical contact lithography with a 365 nm exposure source, followed by photoresist development and a 175 nm partial SiN removal by reactive-ion etching (RIE) with gases  $\text{CF}_4$  and  $\text{H}_2$ , see Fig. 4(b) [11]. Next, a 1.0  $\mu\text{m}$  PECVD  $\text{SiO}_2$  layer is deposited, Fig. 4(c), and planarized by a chemical-mechanical planarization (CMP) process, Fig. 4(d). The interlayer oxide thickness is controlled by measuring the remaining oxide thickness after planarization and depositing a second  $\text{SiO}_2$  layer to achieve a controlled total oxide thickness of 1.00  $\mu\text{m}$ , Fig. 4(e). Then a second 350 nm thick PECVD SiN layer is deposited and patterned in the same way as the first SiN layer, Fig. 4(f).

The same materials and process parameters are used to define both SiN layers. This has the advantage that the effective index of both waveguides in the LCC varies in a similar way for process deviations that affect both SiN layers. As the LCC transmission depends on the effective refractive index difference between the two waveguides [8], the used fabrication process allows to obtain a good control over the LCC transmission.

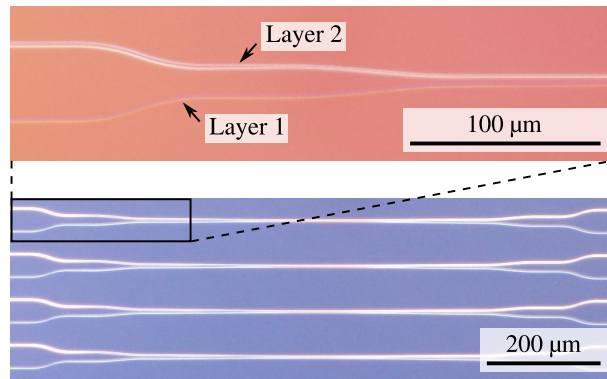


Fig. 3. Optical microscope images of vertical LCCs with indication of the first and second waveguide layer. The apparent width difference between layer 1 and layer 2 waveguides is mostly an artefact from the microscopy.

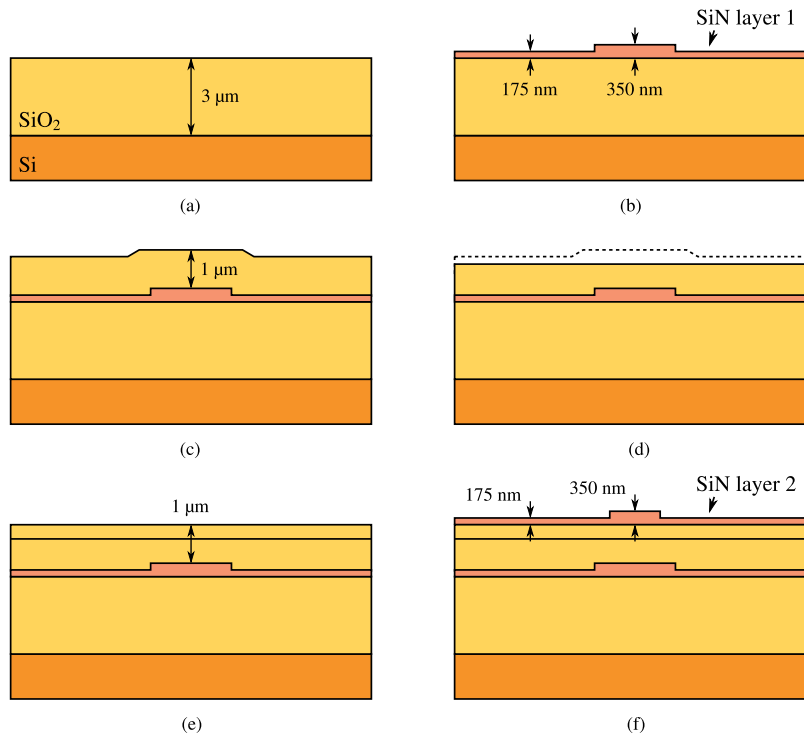


Fig. 4. Fabrication process flow of the vertical LCC; (a) oxidized Si wafer, (b) SiN deposition and patterning, (c) SiO<sub>2</sub> deposition, (d) CMP, (e) SiO<sub>2</sub> deposition, (f) SiN deposition and patterning.

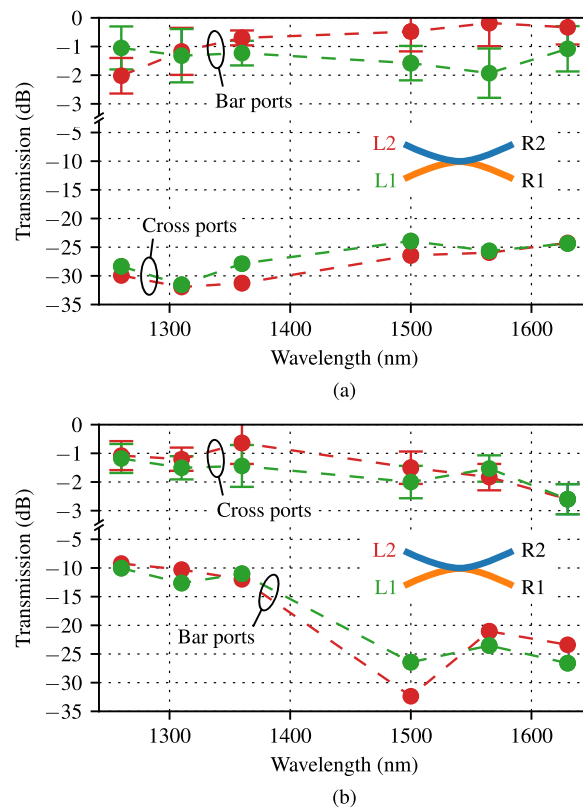


Fig. 5. Measured transmission of a 900  $\mu\text{m}$  long vertical LCC in (a) bar and (b) cross state. The inset shows the port numbers for the upper and lower waveguide. The transmission spectra taken from input ports L1 (lower waveguide level) and L2 (higher waveguide level) are shown in green and red, respectively.

#### 4. Characterization and discussion

The measured transmission of a 900  $\mu\text{m}$  long LCC in bar and cross state is shown in Fig. 5. The fiber-to-chip coupling loss and waveguide loss is excluded from these data points. The waveguide with ports L1 and R1, as shown in the inset of Fig. 5(a), is situated in the first waveguide layer. Similarly, the waveguide with ports L2 and R2 is situated in the second waveguide layer. The bar (L1→R1 and L2→R2) and cross state (L1→R2 and L2→R1) are characterised with liquids that were obtained from Cargille Laboratories [12]. The used liquids have a refractive index of 1.37 and 1.55, respectively, at a wavelength of 1550 nm and at a temperature of 25°C. The liquids were applied to the substrate using a syringe and the substrate was cleaned before switching from one liquid to the other. TE polarized light is coupled into the input waveguide via a lensed fiber connected to tunable Santec laser sources covering the wavelength ranges 1260 nm to 1360 nm and 1500 nm to 1630 nm. The light is coupled out of the output waveguide and is collected by a power meter.

The transmission in Fig. 5 is normalized to the average of 6 reference waveguides in the first SiN layer and 6 reference waveguides in the second SiN layer which are located on the same chip. The length of the error bars in Fig. 5(a) for the transmission between ports L1-R1 and L2-R2 is the standard deviation of the reference waveguides in the first and second layer, respectively. The length of the error bars in Fig. 5(b) for the transmission between ports L1-R2 and L2-R1 is

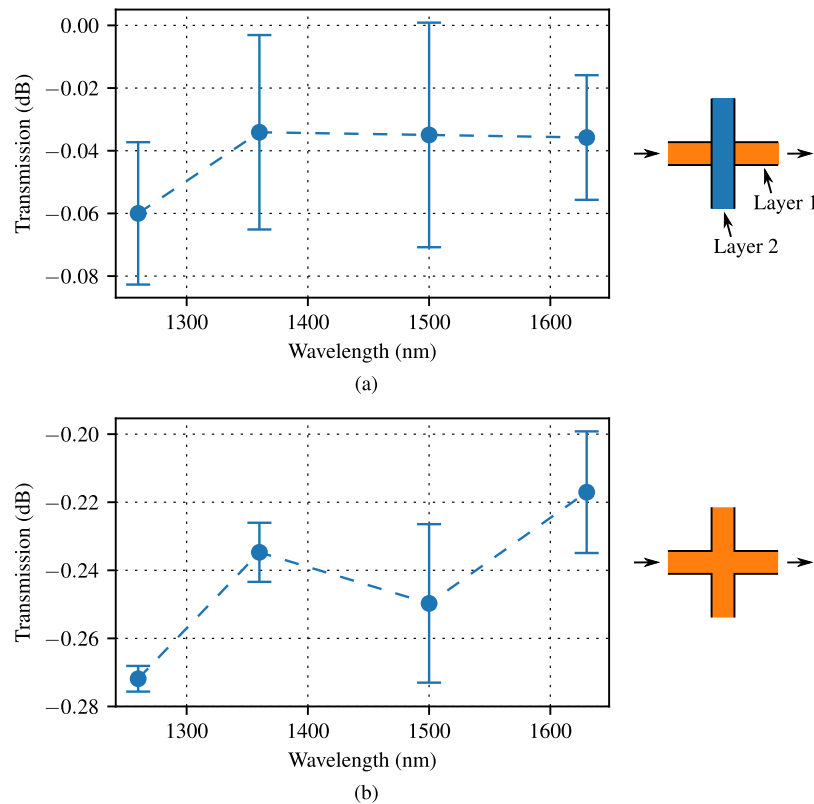


Fig. 6. Measured transmission of a SiN waveguide crossover in (a) 2 waveguide layers and (b) 1 waveguide layer.

the average of the standard deviations of the reference waveguides in the first and second layer. The standard deviations of the reference waveguides are relatively large and could be reduced by using optimized fiber-edge couplers with a reduced reflection. It should be noted that the width of the waveguides in the LCC is different than the width of the reference waveguides. Therefore, the LCC transmission after normalization excludes the waveguide loss only in approximation. The approximation is better when waveguides are used with a transmission that is less dependent on the width such as waveguides with a reduced SiN absorption loss, which can be obtained by low-pressure chemical vapor deposition (LPCVD) or annealing, and waveguides with a reduced roughness.

From Fig. 5 it can be inferred that the IL of the LCC is less than 2.0 dB for the bar state and less than 2.6 dB for the cross state over the full telecommunication wavelength range from 1260 nm to 1630 nm. The XT is less than -24 dB for the bar state over the same wavelength range. For the cross state the XT is less than -21 dB over the wavelength range 1500 nm to 1630 nm and less than -9 dB over the wavelength range 1260 nm to 1630 nm. The measured IL and XT is in general higher than the simulated, except for the XT in cross state between the wavelengths 1260 nm to 1310 nm. It is expected that the performance of the LCC can be further improved by using a more advanced fabrication process that allows a reduced waveguide roughness, sub-micrometer waveguide widths, and an improved control on the waveguide width. Also, the SiN absorption should be reduced, for example by using an LPCVD process.

Building larger switch networks from elementary LCCs typically will require the introduction of waveguide crossovers [13]. The transmission of waveguide crossovers on the same chip in one

waveguide layer and in two waveguide layers is shown in Fig. 6. The waveguide crossovers in a single waveguide layer are situated in the first waveguide layer and have an IL that is less than 0.28 dB. The IL of the interlayer waveguide crossovers is less than 0.06 dB. The transmission per crossover is obtained from a linear regression of the transmission of a waveguide with 0, 1, 10, 20, and 30 crossovers. The standard error of regression is also shown in Fig. 6. The IL and XT of the interlayer waveguide crossover could be further reduced by increasing the interlayer oxide thickness [3]. However, this can also reduce the performance of the LCCs as shown in Fig. 2.

## 5. Conclusion

A vertical liquid controlled waveguide coupler is realized in SiN. The measured IL is less than 2.0 dB for the bar state and less than 2.6 dB for the cross state over the full telecommunication wavelength range from 1260 nm to 1630 nm. The XT of the LCC is less than  $-24$  dB for the bar state over the same wavelength range. For the cross state, the XT is less than  $-21$  dB over the wavelength range 1500 nm to 1630 nm and less than  $-9$  dB over the wavelength range 1260 nm to 1630 nm. We believe the performance of the LCC in terms of insertion loss can be improved by using for example deep-UV lithography, to obtain a better resolution, and LPCVD SiN, to reduce the waveguide absorption loss. Note that using the dilated switch architecture proposed in [13] the high XT in the cross-state no longer impacts the performance of switching networks formed from these elementary switches.

Interlayer waveguide crossovers have a reduced IL compared to planar waveguide crossovers. The IL of the fabricated interlayer waveguide crossovers with the same interlayer thickness as the LCC is less than 0.06 dB over the wavelength range 1260 nm to 1630 nm. This is almost 5 times less than that of a single layer waveguide crossover with the same waveguide width.

By combining vertical LCCs and interlayer waveguide crossovers, large-scale non-volatile switch circuits could be realized with an improved overall performance compared to switch circuits with a single photonic circuit layer.

## Funding

European Union's Seventh Framework Programme SWIFT Project (619643).

## Acknowledgments

The authors would like to thank S. Verstuyft for his help with the fabrication.